Uncertainty of a VHF CubeSat Measurement based on the Synthetic Probe Array Technique

F. Saccardi[1], A. Giacomini[1], R. Tena Sánchez[1], E. Tartaglino[1], P. Moseley[2], L. Rolo[2], L. J. Foged[1]
[1] Microwave Vision Italy SRL, Via dei Castelli Romani 59, 00071, Pomezia, Italy, francesco.saccardi@mvg-world.com
[2] European Space Agency, ESTEC, Keplerlaan 1, 2201 AZ Noordwijk, The Netherlands, Paul.Moseley@esa.int

***Abstract*—In this paper the measurement uncertainty analysis of the radiating tests of the Hera-Juventas CubeSat performed in the indoor HERTZ facility at ESA/ESTEC are presented. The satellite is equipped with a ground penetrating radar mounting two half-wavelength dipoles working in the 50-70MHz band. The nominal lowest frequency of HERTZ is 400MHz hence, to cope with the degraded measurement accuracy at VHF, an ad-hoc measurement solution composed of several "key-components" has been implemented. The synthetic probe array technique, based on the field sampling at different positions generating a virtual array to reduce the illumination of the chamber walls, is the heart of implemented solution. Moreover, the quarter-wavelength averaging technique and the efficiency substitution method, along with RF transparent measurement equipment have also been considered.**

***Index Terms*—synthetic probe array, spherical near field, low frequency, low gain, cubesat, reflections.**

I. Introduction

The Juventas CubeSat of the ESA-HERA mission relies on a low frequency radar equipped with 50-70MHz half-wavelength dipole antennas to study the geophysical properties of a binary asteroid system [1]. The mission requires an accurate verification of the radiation properties of the antenna systems including directivity pattern and gain.

Among different measurement approaches, including outdoor solutions based on drones scanning, the HERTZ testing facility [2] at ESA/ESTEC has been selected for its cost-effectiveness and the possibility to provide repeatable measurements. The anechoic chamber at HERTZ was originally designed for measurements down to 400MHz, hence, its limited electrical size (~5λ x 2λ x 2.5λ at 60MHz) and the poor reflectivity of the absorbers mounted on the walls (~-2dB) give rise to a high reflective environment. To cope with the expected degraded measurement accuracy the so-called Synthetic Probe Array (SPA) technique [3]-[6], along with other system upgrades, including the use of RF transparent antenna positioners [6], have been implemented for such a test campaign.

The effectiveness of the SPA techniques has been verified both by mean of simulations [4] and 10:1 scaled measurements performed in a scenario sufficiently representative of HERTZ [5]. Results in terms of radiation pattern, directivity and gain of the actual measurement campaign in HERTZ have been presented in [6]. In this paper, the analysis performed to derive the uncertainty of such measurement results is presented for the first time.

II. Measurement Solution and Results

The most suited measurement approach for low-gain (omni-like) Devices Under Test (DUT) is the Spherical Near Field (SNF) one because it allows the full 3D pattern characterization without truncation errors [7]-[8]. To cope with the expected degraded accuracy of the SNF system at HERTZ operated at 60MHz, a measurement solution based on several "key-components" described in detail in [6] and briefly recalled here has been implemented.

The "heart" of the implemented measurement solution is the Synthetic Probe Array (SPA) technique [3]-[6], in which a short electric dipole is moved to sample the field in several positions. The subsequent complex superposition of the different measurements is used to synthetize a suitable probe pattern to reduce the illumination of the chamber walls and hence the reflectivity. The considered SPA is a circularly shaped lattice of 1λ diameter at 60MHz. Two array layers (with 13 positions each) are considered to reduce the illumination of the probe backwall. Instead, to cope with the reflections from DUT backwall (where most of the power is directed), the λ/4-averiging technique [9], based on the measurement of the DUT at two positions λ/4 away from each other, has been considered.

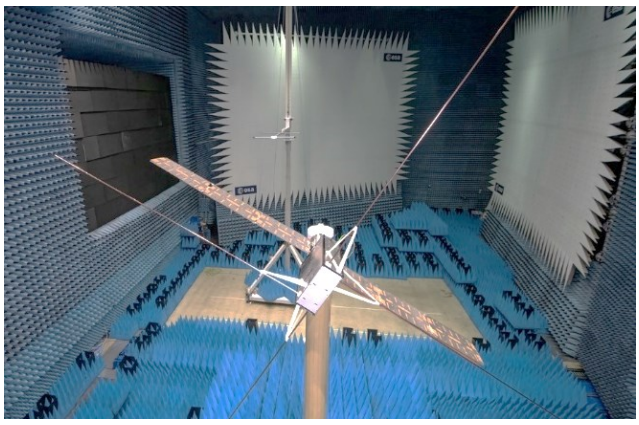

Fig. 1. Juventas CubeSat installed in the HERTZ facility at ESTEC [2].

As concern the gain calibration, the efficiency substitution method [7], [10] has been implemented. As pointed out in [10], considering the efficiency of the reference antenna, instead of the gain, allows to further reduce possible error due calibration. In this case, a λ/2-dipole, previously characterized

with the Wheeler-cap method [11], has been considered as reference antenna. The similarity of such antenna with the actual DUT, allows to further reduce the uncertainty as they would likely experience the same errors, which will tend to cancel out.

Another important aspect is of course the interaction with the measurement equipment such as DUT/probe supporting structures and cables. A roll-over-azimuth DUT positioner with a RF transparent mast (i.e. Kevlar material) has been specifically designed and manufactured for this test campaign. Similarly, a fiberglass probe positioner allowing the X,Y,Z degrees of freedom required to realize the SPA has been designed and installed in the chamber at approximately 8m from the DUT. Due to the large 3D positioning footprint, RF transparency requirements, reversible installation, and cost constraints, a manually driven solution has been selected for this positioner [6]. Finally, to avoid unbalanced currents on the feeding lines, that would excite unwanted, interfering radiations, RF-to-optical transducers and optical fibers have been used both on the DUT and on the probe side.

Measurement results from such an implemented solution in HERTZ are described in detail [6] and here briefly recalled. In Fig. 2 the radiation patterns of the Juventas Cubesat measured with the implemented SPA-based technique and the conventional single probe approach are reported. As can be seen the former is in much better agreement with the theoretical λ/2-dipole model than the latter, highlighting the effectiveness of implemented technique. Peak directivity and gain results are also recalled and shown in Fig. 3.

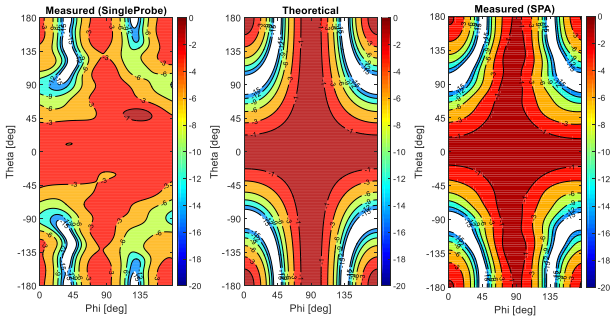

Fig. 2. Copolar pattern of Juventas cubesat at 60MHz: measured in HERTZ and compared with the theoretical model of a λ/2-dipole.

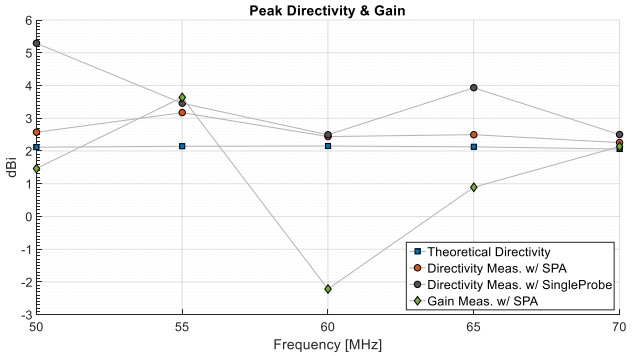

Fig. 3. Comparison of peak directivity and gain over frequency.

III. Directivity Uncertainty

The directivity uncertainty of the Juventas CubeSat measured in HERTZ with the implemented technique has been evaluated considering the well-known NIST 18-term error list [12]. Even though such a list is meant for planar near field measurements, it has been considered here, adapting some terms to this specific measurement scenario. The derived error budget is reported in TABLE I.

TABLE I. Estimated Directivity Uncertainty

Id	Error Source	Error 1σ [dB] In band	Error 1σ [dB] Out of band
1	Probe relative pattern	0.06	0.06
2	Probe polarization ratio	0.00	0.00
3	Probe gain	-	-
4	Probe alignment	0.00	0.00
5	Normalization constant	-	-
6	Impedance mismatch	-	-
7	AUT alignment error	0.05	0.05
8	Aliasing error	0.00	0.00
9	Truncation error	0.00	0.00
10	Probe X, Y positioning errors	0.01	0.01
11	Probe Z positioning errors		
12	Probe / AUT mutual coupling	0.01	0.02
13	Receiver amplitude linearity	0.01	0.01
14	System phase error	0.01	0.01
15	Receiver dynamic range	0.03	0.03
16	Chamber effect (scattering)	0.27	0.48
	Chamber effect (ML variation)	0.03	0.15
17	Leakage and crosstalk	0.00	0.00
18	Random amplitude/phase errors	0.00	0.00
	Total Uncertainty (RSS, 1σ)	0.29	0.51
	Total Uncertainty (RSS, 2σ)	**0.57**	**1.01**

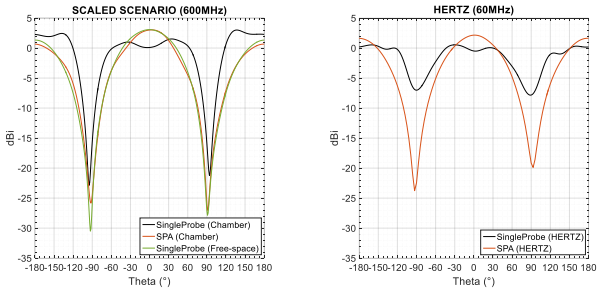

Fig. 4. Comparison of directvivity patterns obtained from the scaled scenario and the real measurents at HERTZ.

Despite the adoption of the SPA and λ/4-avering techniques, to chamber effect due to the reflections is still the dominant term (see term #16). The residual error due to the chamber effect has been evaluated considering the 10:1 scaled measurement described in detail in [5]. Such scaled measurements were performed prior the actual measurements in HERTZ to experimentally validate the SPA technique in a realistic test environment where it was possible to remove the effect of the chamber and get a (quasi) free space reference data (see more details in [5]). To use the outcomes of such a scaled experiment as estimator for chamber reflection term of the actual measurements in HERTZ, the similarity of the two measurement environments has been checked. The directivity radiation patterns of the λ/2-dipole measured in the 10:1 scaled scenario at 600MHz are shown on the left side of Fig.

4, while the those of the Juventas cubesat measured in HERTZ at 60MHz on the right side of the same figure. In both graphs the black traces are obtained with the conventional single probe approach while the orange ones with the SPA technique. The patterns obtained in the two ranges are in good agreement meaning that the implemented scaled scenario was indeed a good approximation of the HERTZ facility, allowing the use of the former to estimate the uncertainty term due to the chamber reflections.

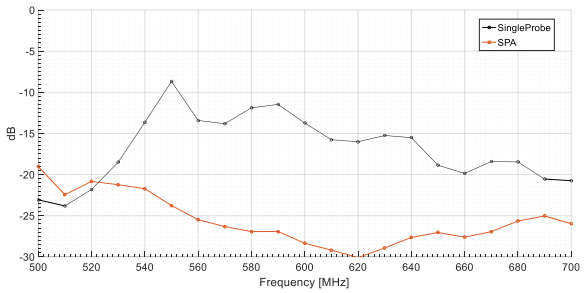

Fig. 5. ENL from the scaled measurement scenario (free space measurement is used are reference).

From the scaled measurements, the Equivalent Noise Level (ENL), defined in equation (1)

$$ENL = 20\log_{10}\left(RMS\left|\frac{E(\theta,\,\varphi) - \tilde{E}(\theta,\,\varphi)}{E(\theta,\,\varphi)_{MAX}}\right|\right) \qquad (1)$$

is computed and shown in Fig. 5 for each tested frequency. In such a metric $E(\theta,\,\varphi)$ is the reference radiation pattern, which is the (quasi) free space scaled measurements (see green trace in Fig. 4 as an example). $\tilde{E}(\theta,\,\varphi)$ instead, is the perturbed pattern, which in this case are the ones obtained from the conventional single probe acquisition and the SPA technique. It should be noted that, since the reference free space measurement was performed under the same conditions of the one inside the chamber (e.g. same positioners, same cables, etc… [5]), these error levels are mainly associated only to the effect of the chamber itself. It is recalled that the worse performance below 550MHz, were due to a poor F2B of the scaled probe [5], hence only the 550-700MHz band is considered in this case, where the ENLs vary from -25dB to -30dB approximately. It should be noted that the lowest values are obtained close to the resonant frequency of the considered dipole antenna, suggesting different performance of the technique at "in band" (close to 60MHz) and "out of band" frequencies. From the ENL, equation (2) is used to obtain the uncertainty at 0dB Antenna Pattern Level (APL).

$$\varepsilon = 20log_{10}\left(1 + \frac{10^{ENL/20}}{10^{APL/20}}\right) \qquad (2)$$

In particular, an ENL of -30dB and -25dB have been considered respectively at "in band" and "out of band" frequencies, corresponding to 0.27dB and 0.48dB of 1σ-uncertainty (i.e. 1σ because the Root Mean Square, RMS, is considered in the ENL metric).

Another error source associated with the chamber effect is the variation of Mismatch Losses (ML) of the test antenna. Of course, the matching of the antenna should not change during test, but unfortunately, already in the preliminary analysis of this project, it has been found that the interaction of the antenna with the environment (e.g. also including the positioners) at such low frequencies has an effect also on the matching. It should be noted that such unwanted effect is not mitigated by the SPA technique, hence it must be accounted for in the uncertainty budget.

The peak-to-peak variation of the ML, obtained by measuring the return loss at several antenna orientations, is shown on the left side of Fig. 6, for both the scaled and actual HERTZ scenarios. As expected, in both cases the lowest variations are observed close to the resonant frequency. Moreover, at non-resonant frequencies, such effect is significantly more pronounced in the actual HERTZ scenario hence the additional term "Chamber effect (ML variation)" has been included in the uncertainty budget. The ML effect on the final radiation pattern has been evaluated by emulating SNF measurements (i.e. with the spherical wave-based transmission formula [8]) of a λ/2-dipole including the measured ML variation and performing the NF/FF transformation. Beside the amplitude variation due to the ML, a maximum phase variation of 1° has been also estimated from the measurement of the return loss of the reference antenna in HERTZ. Such phase variation has also been included in the measurment emulation, on top of the ML effect. The achieved ENL around the resonant frequency is approx. -50dB while at out of band frequencies is -35dB at worst. These two error levels give rise to a 1σ-uncertainty of 0.03dB and 0.15dB respectively in band and out of band as shown in TABLE I.

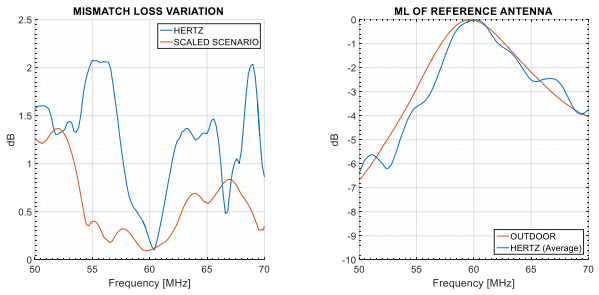

Fig. 6. ML variation of the reference antenna measured in HERTZ and in the scaled scenario considering different antenna orientations (left); comparison of the ML of the reference antenna measured outdoor and in HERTZ by averaging the different antenna orientations (right).

Even though a much less significant contribution was expected from the other uncertainty terms, they also have been evaluated for completeness (all except terms #3, #5 and #6 which do not affect the directivity).

Term #1 accounts for the influence of the pattern of the synthetic probe array (1λ diameter) used to mitigate the chamber effect. Theoretically, the probe pattern compensation should be applied to avoid a distortion of the measured DUT pattern [8]. Practically, since an onset and electrical small

DUT is measured, this error term is expected to be relatively low. Nevertheless, such an effect has been evaluated performing SNF measurements emulations of a λ/2-dipole considering as probe the theoretical model of the SPA. The obtained errors are in line with the expectations (TABLE I).

Similar measurement emulations have been performed to estimate the effect of the X, Y, Z positions error of the SPA. From the manual movements of the dipole used to generate the SPA in the range, +/-2cm (+/-0.004λ at 60MHz) error in all the directions has been estimated as worst case assumption. With this input, uniformly distributed random variations of the array lattice has been considered in the measurement emulations, obtaining the errors reported in TABLE I (see terms #10 and #11). Repeatability tests have also been performed before starting the actual measurements observing a maximum variation at the peak of the near field of 0.1dB. Such variation is expected to be reduced by the averaging effect of the synthetic probe array and the NF/FF transformation. Hence, the estimated value for this error term is also in line with the expectations.

It is known that probe polarization ratio and alignment (see term #2 and #4) have usually a negligible contribution on the directvity measurement of electrically small antennas. This assumption has been verified again with measurement emulations, considering a probe cx-polar of -30dB and an alignment error of 1°.

Concerning the alignment of the DUT (term #7), some vibrations have been observed during the spherical scanning. Dedicated onsite tests showed that these vibrations generate no more than 0.1dB fluctuations at the measured peak of the signal. This error has been modelled with simulations by adding a Gaussian noise of -40dB to the emulated near field and checking the results after the data transformation.

Aliasing and truncation errors (see terms #8 and #9) have both been considered negligible since a full sampling based on the electrical size of the DUT [8] has been considered and a complete SNF acquisition has been performed.

The DUT-probe mutual interaction (term #12) has been investigated with full-wave simulations where the coupling between a λ/2-dipole and a short electric dipole was simulated varying the distance. The obtained low contribution was expected given the electrical sizes of the two antennas. The considered out of band value accounts for a significantly worse matching of the DUT (i.e. -1dB return loss assumed).

Amplitude linearity and system phase errors (terms #13 and #14) have been evaluted by checking the responses of the RF-optical converters and fibers before the actual campaign at HERTZ. By varying the input power, a maximum variation of 0.1dB was observed, generating an ENL of approx. -60dB after the NF/FF transformation. Moreover, "stress tests" of the optical fibers allowed to verify a maximum phase variation of +/-0.1°. On top of it, the phase error of the rotary joint has been added for a total of +/-0.2°, giving rise to a maximum ENL of -56dB after the NF/FF transformation.

The dynamic range of the implemented measurement setup at HERTZ was approx. 50dB, hence term #15 has been estimated considering an ENL of -50dB.

The last two terms of the NIST 18-term list have been considered negligible given that no criticalities regarding the leakage or crosstalk have been observed during the whole measurement campaign. Moreover, possible contributions due to random amplitude/phase error can be considered included in the term #16.

The resulting directivity uncertainties (obtained with the Root Square Sum, RSS, of all the terms) are smaller than the required ones, being +/-1dB (2σ). With reference to Fig. 3, it should be noted that the deviations of the measured directivity of the DUT with respect to the theoretical directivity of a λ/2-dipole are within the estimated uncertainty. It is finally highlighted that if the conventional single probe approach was used, the uncertainty would have been approx. +/-3dB (2σ).

IV. GAIN UNCERTAINTY

The gain of the Juventas CubeSat (G_{DUT}) has been measured with the efficiency substitution technique [7], [10], hence using the calibration equation (3) below,

$$G_{DUT} = \eta_{REF} \frac{|w_{DUT}|^2}{\eta_{REF,RAW}} \tag{3}$$

where $|w_{DUT}|^2$ is the peak of the radiation pattern obtained from the SNF measurements, η_{REF} is the efficiency of the reference λ/2-dipole antenna measured with the Wheeler-cap technique [11], and $\eta_{REF,RAW}$ is the (raw) efficiency of the same reference antenna measured in HERTZ with the implemented technique. Since three terms are involved in the gain determination, the uncertainty of each one is considered and then combined with the RSS (see TABLE II.).

TABLE II. ESTIMATED GAIN UNCERTAINTY

Id	Error Source	Error 1σ [dB]	
		In band	Out of band
1	DUT pattern	0.29	0.51
2	Reference efficiency	0.10	0.20
	Meas. efficiency (scattering)	0.07	0.15
3	Meas. efficiency (ML variation)	0.04	0.09
	Meas. efficiency (ML absolute)	0.25	0.50
	Total Uncertainty (RSS, 1σ)	0.40	0.76
	Total Uncertainty (RSS, 2σ)	**0.80**	**1.52**

The uncertainty of the $|w_{DUT}|^2$ term is basically the one with which the DUT pattern is measured, hence it is estimated considering the directivity uncertainty previously computed.

The uncertainty of the reference efficiency (term #2) depends on the accuracy of the Wheeler-cap method used to measure it. The Wheeler-cap method is known to be very accurate at the resonance frequency. In this case, the Wheeler enclosure, has been designed for this specific antenna at 60MHz [6]. The measured efficiency at 60MHz matched well the expected values so that a 1σ-uncertainty of 0.1dB can be estimated. For the out of band frequencies, a similar accuracy is expected. Nevertheless, it has been assumed that the Ohmic losses measured at 60MHz are the same in the whole 50-70MHz. This is a reasonable assumption, but the associated uncertainty is higher (e.g. 0.2dB).

As concern the uncertainty of the efficiency of the reference antenna measured in HERTZ (term #3) three factors have been identified, namely: the room scatting, the ML variation and the absolute ML error.

For the first one, the efficiency errors obtained in the scaled experiment are considered (see details in [6]). Close to the resonant frequency a maximum error of 0.2dB was observed, which translate to a 1σ-uncertainty of 0.07dB (assuming a Gaussian distribution). Similarly, outside the central frequency, the maximum error was 0.4dB, hence approx. 0.15dB (1σ). It is pointed out that such efficiency errors were found assuming a high similarity between the (scaled) DUT and reference antenna. In the actual measurements in HERTZ both the DUT and the reference antenna are basically λ/2-dipoles hence the same assumption can be considered valid.

The effect on the measured efficiency due to the variation of the ML has been evaluated from the same ML measurements done in HERTZ, shown on the left side of Fig. 6 and the same measurement emulations considered for the corresponding error term of the directivity uncertainty. As can be seen in TABLE II, this achieved uncertainty term is relatively low, remarking the effectiveness of the efficiency substitution technique, which allows to average out possible fluctuations in the measured radiation pattern [10].

Finally, the last term accounts for a possible global offset of the matching of the reference antenna when installed in final measurement environment. To quantify this error term the ML of the reference antenna have been characterized in HERTZ with measurements performed at several orientations which have then been averaged. The achieved ML are compared to those of the same antenna measured outdoor, prior the test campaign in HERTZ (see right side of Fig. 6). The reported 1σ-uncertainties in TABLE II. , are obtained from the difference between the ML measured in two different environments. It should be noted that to be on the "safe side" this error term should be considered twice if the reference and test antennas cannot be assumed sufficiently "similar". On the other hand, very similar antennas would likely experience the same errors, which will tend to cancel out. In this analysis it has been decided to stay "half way" between the two extreme situations, considering this term only once. It is also highlighted that the ML differences observed in the right side of Fig. 6 could have been reduced including measurement performed at two positions λ/4 away from each other in the average. Since these measurements are included in the implemented solution (i.e. λ/4-averaging technique), the last estimated uncertainty term can be considered a worst-case.

The total gain uncertainty, obtained with the RSS of each term, are much smaller than the required ones, being +/-2dB (2σ). As for the directivity, it should be noted that the conventional single probe approach would have led to an uncertainty of +/-3dB (2σ).

V. Conclusions

The measurement uncertainty of the radiating test of the Hera-Juventas CubeSat performed in the HERTZ facility at ESA/ESTEC has been reported in this paper. To cope with the expected high reflective environment at the frequencies of interest (50-70MHz), the synthetic probe array technique has been implemented along with other specific techniques and measurement equipment (λ/4-averaging technique, efficiency substitution method, RF transparent positioners and optical links). The directivity uncertainty has been evaluated adapting the well-known NIST 18-term list to this specific measurement scenario. For the gain instead, the uncertainty of each term involved in the substitution method has been considered. Despite the implemented measured solution, the chamber effect is still the main contributor to the global uncertainty, nevertheless, it has been shown that both the directivity and gain uncertainties are well within the requirements, being respectively +/-1dB and +/-2dB (2σ).

An analog plane wave generator would be a logical evolution of the implemented solution since it allows to reduce the interaction with the environment and to enforce a far field condition, enabling direct end-to-end tests [13].

Acknowledgment

The activities reported in this paper have been carried out under a program of and funded by the ESA.

References

[1] https://www.heramission.space/hera-mission-juventas-cubesat

[2] https://www.esa.int/Enabling_Support/Space_Engineering_Technology/Test_centre/Antenna_Test_Facilities

[3] J. Knapp and T. F. Eibert, "Accurate determination of radiation patterns from near-field measurements in highly reflective environments" EuCAP 2018, 9-13 April, London, UK.

[4] R. Tena Sánchez, et al. "Near-Field Measurement Technique for Spacecraft Installed Low Frequency Antennas" AMTA 2021, October 24-29, Daytona Beach, FL, USA

[5] R. Tena Sánchez, et al. "Measurement of Low Frequency Antennas in Indoor Reflective Environments with the Synthetic Probe Array Technique", EuCAP 2022, 27March – 1 April 2022, Madrid, Spain

[6] F. Saccardi, R. Tena-Sanchez, E. Tartaglino, A. Giacomini, L. J. Foged P. Moseley, L. Rolo "Testing of a 60 MHz Cubesat in an Electrically Small Environment with the Synthetic Probe Array Technique", AMTA 2022, October 9-14, Denver, CO, USA

[7] IEEE Std 1720-2012 "Recommended Practice for Near-Field Antenna Measurements"

[8] J. E. Hansen (ed.), Spherical Near-Field Antenna Measurements, Peter Peregrinus Ltd., on behalf of IEE, London, United Kingdom, 1988

[9] L. J. Foged and others, ACE2 deliverable A1.2D2, "Recommendations and comparative investigations for near-field antenna measurement techniques and procedures", Dec 2007

[10] F. Saccardi, et al., "Accurate Calibration of Truncated Spherical Near Field Systems with Different Ground Floors using the Substitution Technique" AMTA 2019, October 6-11, San Diego, USA

[11] H. A. Wheeler, "The Radiansphere around a Small Antenna", Proceedings of the IRE, pp. 1325-1331, August 1959.

[12] A. C. Newell, "Error analysis techniques for planar near-field measurements," in IEEE Transactions on Antennas and Propagation, vol. 36, no. 6, pp. 754-768, June 1988, doi: 10.1109/8.1177.

[13] F. Saccardi, R. Tena-Sanchez, E. Tartaglino, A. Giacomini, L. J. Foged, P. Moseley, L. Rolo "Measurement of VHF Satellite Antennas using the Synthetic Probe Array Technique" Internation Symposium on Measurements and Networking, Padua, Italy, 18-20 July, 2022